J Appl Electrochem (2008) 38:1677–1681
DOI 10.1007/s10800-008-9616-1

ORIGINAL PAPER

Manganese oxide precipitated into activated carbon electrodes for electrochemical capacitors

Chuen-Chang Lin · Chia-Cheng Yen

Received: 18 August 2006 / Accepted: 30 May 2008 / Published online: 17 June 2008

Abstract Manganese oxide was prepared at different pH and temperatures and then precipitated into activated carbon by the chemical impregnation method. Size distributions of manganese oxide sol were also measured by light scattering. The electrodes were annealed in nitrogen gas at different temperatures. In addition, electrochemical characterization was carried out using cyclic voltammetry (CV) at a scan rate of 25 mV s^{-1} and chronopotentiometry (CP) with constant-current (10 mA cm^{-2}). Maximum capacitance of 461.3 F g^{-1} was obtained in a 0.1 M Na_2SO_4 solution for manganese oxide prepared under optimum conditions (pH = 13.11 and T = 25 °C) and annealed at a temperature of 195 °C. The manganese oxide particle size decreased with annealing. This probably leads to increased specific capacitance. Using X-ray photoelectron spectroscopy (XPS) the results reveal that manganese oxide species are transformed from hydroxide to oxide after annealing.

Keywords Manganese oxide · Chemical impregnation · Annealing · Scanning electron microscope · Electrochemical capacitors

1 Introduction

Electrochemical capacitors are charge-storage devices, which possess higher power density and longer cycle life than batteries [1–3]. Their applications include hybrid power sources, backup power sources, starting power for fuel cells, and burst-power generation in electronic devices [4–8]. Electrochemical capacitors are classified into two types, electric double layer capacitors (EDLC) and pseudocapacitors according to the energy-storage mechanisms. The capacitance of EDLC arises from the separation of charge at the interface between the electrode and the electrolyte. However, pseudocapacitance arises from redox reactions of electroactive materials with several oxidation states [1, 9–13].

Amorphous hydrous ruthenium oxide prepared by the sol–gel method has been found to possess very high specific pseudocapacitance value of 720 F g^{-1} [14]. However, the precursor of hydrous ruthenium oxide is very expensive. Hence, the more economical manganese oxide appears to be a promising electrode material for electrochemical capacitors. Recently, manganese oxides were prepared by different methods for their applications as electrode materials in electrochemical capacitors. A thin film of manganese oxide prepared by the dip-coated sol–gel derived technique involving $KMnO_4$ and $MnCl_2$ was found to exhibit high specific capacitance of 698 F g^{-1} (at a scan rate of 5 mV s^{-1} and in 0.1 M Na_2SO_4) and long cycle life. However, the discharge time is only about 1.1 s at constant current of 0.1 mA and the slope of the constant current discharge curve is not exactly constant [15]. In addition, pure amorphous hydrous manganese oxide prepared by the co-precipitation method involving $KMnO_4$ and $Mg(CH_3COO)_2$ reduced capacitive response rate because of the relatively high resistance of manganese oxide and co-precipitated carbon-amorphous hydrous manganese oxide possessed specific capacitance of 144 F g^{-1} [16]. Moreover, the ambigel form of manganese oxide synthesized by the sol–gel method reducing $NaMnO_4$ with $Na_2C_4H_2O_4$ offered maximum capacitance of 130 F g^{-1}, at a scan rate of 5 mV s^{-1} and in 2 M NaCl solution [8]. Therefore, manganese oxide was

C.-C. Lin (✉) · C.-C. Yen
Department of Chemical & Materials Engineering, National Yunlin University of Science and Technology, 123 University Road Sec. 3, Douliu, Yunlin 64002, Taiwan, ROC
e-mail: linchuen@yuntech.edu.tw

prepared at different pH and temperatures then precipitated into activated carbon by the chemical impregnation process and annealed at different temperatures. Furthermore, the surface morphology, chemical environment and crystalline structure of the activated carbon electrode were examined by scanning electron microscopy (SEM), X-ray photoelectron spectroscopy (XPS) and X-ray diffractometry (XRD).

2 Experimental methods

Manganese oxide sol was prepared by reduction of $KMnO_4$ with $MnSO_4H_2O$ [17]. NaOH was added to $KMnO_4$ to produce a 500 mL solution of 8×10^{-5} M MnO_4^- solution at different pH (10.5–13.11). To the vigorously stirred $KMnO_4$ solution, 7.5×10^{-2} M $MnSO_4H_2O$ (800 μL) was then rapidly added by micropipette at different temperatures (15–55 °C). This procedure produced a transparent yellow brown sol within several seconds. Size distributions of manganese oxide sol were measured by light scattering using a particle size analyzer system (Brookhaven Instruments, model: 90 Plus).

Next, because of its higher specific surface area, lower specific resistance, a higher percentage of mesopore size distribution, and cheaper, activated carbon was weighed and put into a three-necked flask. The flask was put under vacuum at 95 °C then cooled in air and kept under vacuum. Manganese oxide sol was injected into the flask for coating. In order to allow complete absorption of the sol by the activated carbon, the flask was continuously shaken. Finally, the activated carbon coated with manganese oxide was dried for 2 h at 95 °C and then re-weighed.

About 1.7 g of the activated carbon coated with manganese oxide was completely mixed with 0.3 g of PVDF (polyvinylidenefluoride) binder and 3.5 mL of NMP (*N*-methyl-2-pyrolidinone) solvent for 10 min, and then shaken ultrasonically for 20 min to completely remove any bubbles formed by stirring. Next, the mixed sludge of electrode material was homogeneously spread on stainless steel mesh (about 1 cm^2) by means of a knife blade to an approximate thickness of 1 mm. The mesh had previously been rinsed ultrasonically with acetone, etched in 6 M aqueous HCl for 30 min at 75 °C to increase its surface roughness, rinsed ultrasonically with deionised water and then dried in air and weighed. Finally, the prepared electrodes were dried for 8 h at 90 °C, weighed and then annealed in nitrogen gas for 5 hr at various temperatures (130–220 °C) under a temperature increment rate of 3 °C min^{-1}.

The electrochemical measurements for the prepared electrodes were performed by an electrochemical analyzer (CH Instruments CHI 608B, USA). The three-electrode cell consisted of Ag/AgCl as the reference electrode, Pt as the counter electrode and the prepared electrodes as the working electrode. The electrolytes were degassed with purified nitrogen before voltammetric measurements and nitrogen was passed over the solution during all measurements. The solution temperature was maintained at 25 °C by means of a circulating water thermostat (HAAKE DC3 and K20, Germany). The CV was undertaken with aqueous Na_2SO_4 due to a decrease in the equivalent conductivities of neutral electrolytes (without corrosion and smaller radius of hydration sphere of ions [8, 18, 19]) in aqueous solutions in the order $Na_2SO_4 > KC1 > NaC1 > LiC1$ [20]. CP was carried out at a current density of 10 mA cm^{-2}. A CV scan rate of 25 mV s^{-1} in the range 0–1 V was used in all measurements except where stated. Specific capacitance (F g^{-1}) is normalized to 1 g of manganese oxide except where stated.

Particle size and surface morphology of the electrode materials were analyzed using a JEOL JSM35 SEM. XRD (SIEMENS Rigaku D5000, Germany) using a Cu target was used to characterize the crystalline structure of the electrode material. The chemical environment of the electrode material was explored by XPS (VG Scientific ESCA 250, England).

3 Results and discussion

Manganese oxide sols were prepared for precipitated into activated carbon from reduction of $KMnO_4$ with $MnSO_4H_2O$ at different pH values (10.5, 12.4, and 13.11) and temperatures (15, 25, 35, and 55 °C). Effective diameters of manganese oxide sols as measured by light scattering are presented in Tables 1 and 2 which shows that the higher the pH, the smaller the effective diameter of manganese oxide sol; and the higher the temperature, the larger the effective diameter of manganese oxide sol except at 15 °C. Similar results have been published previously [21]. These also mention that a transparent brown MnO_2 sol was stable at high pH. At pH = 13.11 and T = 25 °C, the effective diameter of manganese oxide reached a minimum of 183.5 nm. The curves in Fig. 1a and b show that there are two groups of size distributions of manganese oxide sol. One is a larger size distribution (470–1,070 nm) (See Fig. 1a) of manganese oxide sol due to some clustering of the primary particles, and another is a smaller size distribution (8–18 nm) (See Fig. 1b). This observation is confirmed in the literature [17].

Figure 2 shows the effects of pH and temperature on the specific capacitance, which reached a maximum at optimum conditions (pH = 13.11 and T = 25 °C). The higher the pH, the higher the specific capacitance; and the higher the temperature, the lower the specific capacitance except at 15 °C due to the larger effective diameter of manganese oxide sol synthesized at too low a temperature of 15 °C

Table 1 Effective diameters of manganese oxide sol (prepared at different temperatures and pH = 13.11) measured by light scattering

Temperature (°C)	15	25	35	55
Effective diameter (nm)	257.1	183.5	384.6	411.7

Table 2 Effective diameters of manganese oxide sol (prepared at different pH and T = 25 °C) measured by light scattering

pH	10.5 ± 0.1	12.4 ± 0.1	13.11 ± 0.1
Effective diameter (nm)	288.2	200	183.5

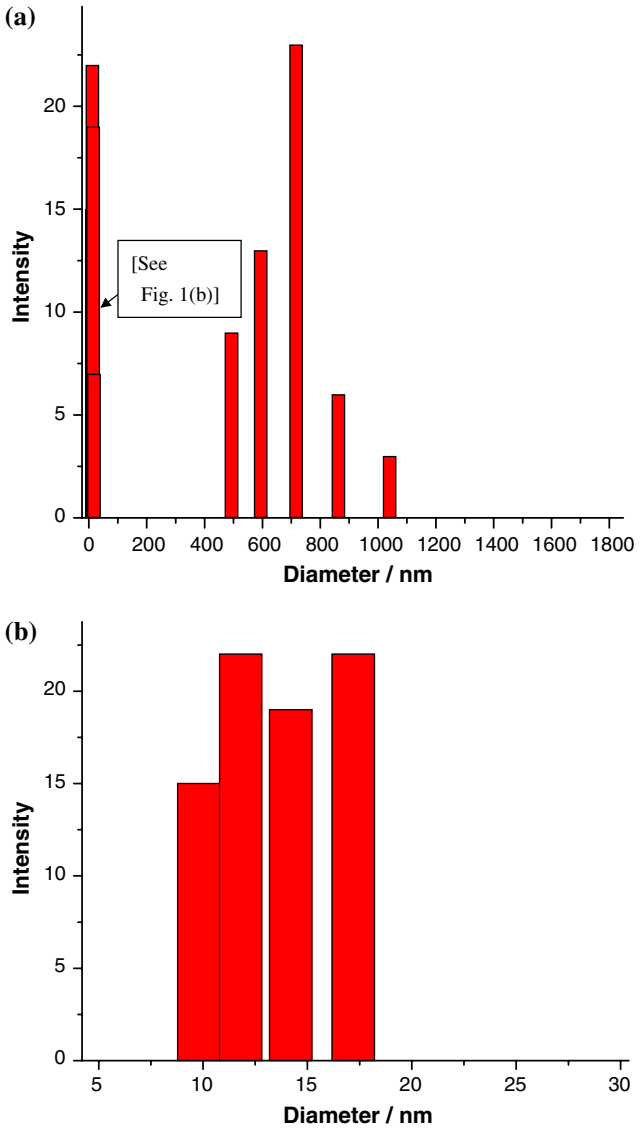

Fig. 1 (**a**) Size distribution of manganese oxide sols prepared under optimum conditions as measured by light scattering. (**b**) Size distribution (8–18 nm) of manganese oxide sols prepared under optimum conditions as measured by light scattering

(See Table 1). Maximum specific capacitance and minimum effective diameter of manganese oxide was achieved under the same conditions (pH = 13.11 and T = 25 °C)

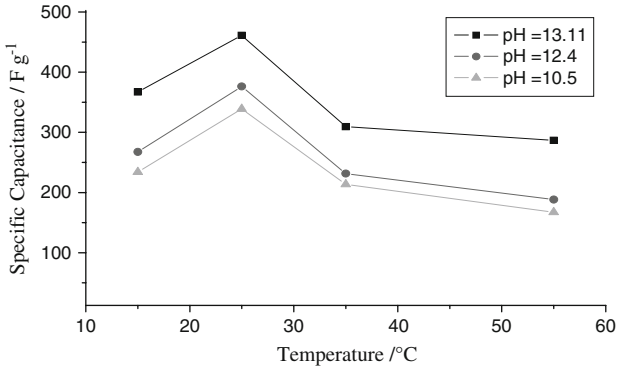

Fig. 2 Effects of pH and temperature of preparation of manganese oxide annealed at 195 °C on the specific capacitance in 0.1 M Na_2SO_4 electrolyte

for preparation of manganese oxide sol. Thus, smaller effective diameter gives higher specific capacitance. The reason behind this behaviour may be that the smaller is the effective diameter, the higher is the specific area and the more numerous the potentially electroactive sites, leading to higher specific capacitance.

Figure 3 shows the effect of annealing temperatures (130, 160, 195, and 220 °C for 5 h under nitrogen at 3 °C min^{-1}) on specific capacitance, which reached a maximum (461.3 F g^{-1}) at 195 °C.

From Fig. 4, the specific capacitance of the electrode (manganese oxide prepared under optimum conditions and then annealed at 195 °C) decreased with increasing number of charge–discharge cycles during the first 100 cycles, but remained almost constant after 100 cycles. This may be attributed to loss of electroactive material through partial dissolution or detachment (electrolyte color changed from transparent to turbid) during the early charge–discharge cycles. Figure 5 shows CP of the optimum electrode with a

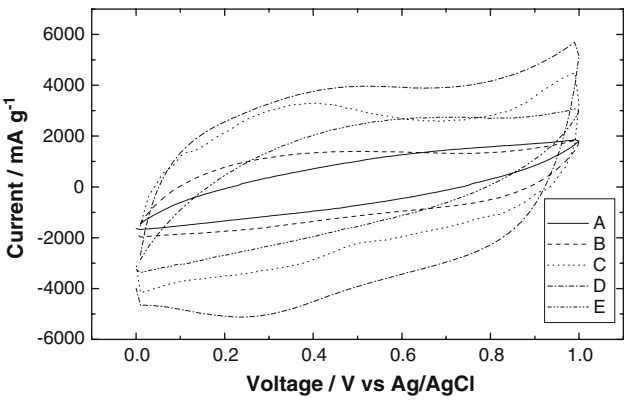

Fig. 3 Effect of annealing temperature on the specific capacitance [manganese oxide prepared under the optimum conditions, A (without annealing): 109.7 F g^{-1}, B (T = 130 °C): 271.1 F g^{-1}, C (T = 160 °C): 357.5 F g^{-1}, D (T = 195 °C): 461.3 F g^{-1}, and E (T = 220 °C): 307.7 F g^{-1}] in 0.1 M Na_2SO_4 electrolyte

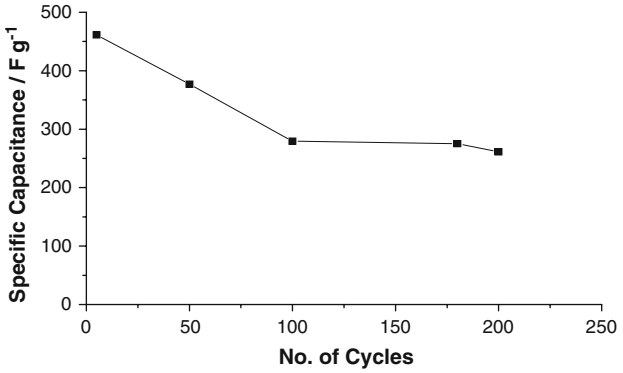

Fig. 4 Effect of number of charge–discharge cycles on specific capacitance for the electrode (manganese oxide prepared under optimum conditions and then annealed at 195 °C) in 0.1 M Na_2SO_4 electrolyte

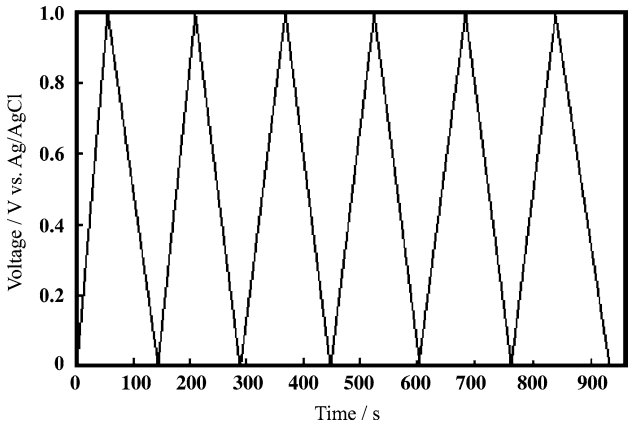

Fig. 5 CP of the electrode (manganese oxide prepared under the optimum conditions and annealed at 195 °C) with a constant current density of 10 mA cm^{-2} in 0.1 M Na_2SO_4 electrolyte

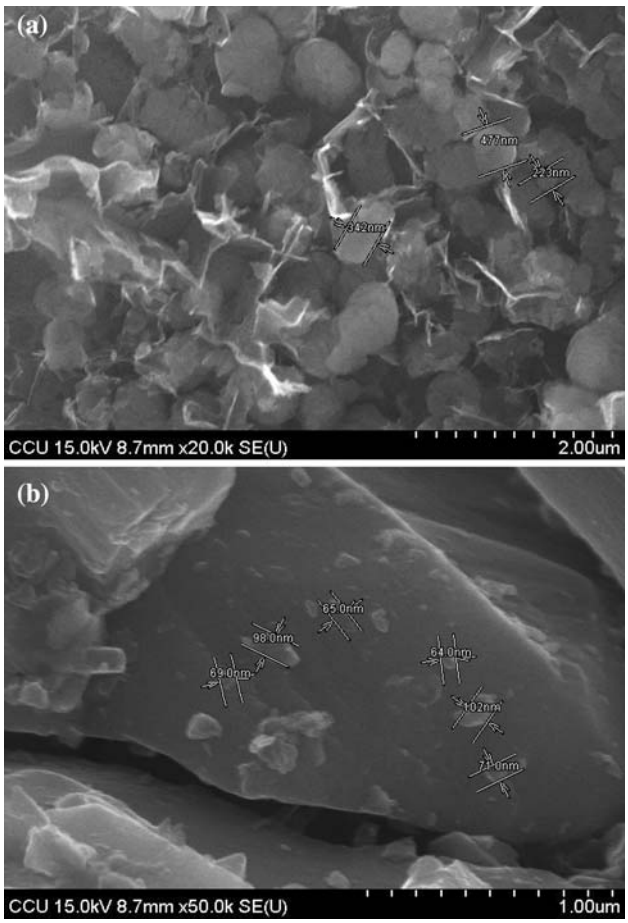

Fig. 6 (**a**) SEM picture of the electrode (manganese oxide prepared under the optimum conditions) without annealing. (**b**) SEM picture of the electrode (manganese oxide prepared under optimum conditions) with annealing at 195 °C

constant current density of 10 mA cm^{-2}. Its charge and discharge curves were symmetrical and similar. This demonstrates that the optimum electrode has high electrochemical reversibility.

The particle size and surface morphology of the electrodes (manganese oxide prepared under optimum conditions) without annealing and with annealing at 195 °C are shown in Fig. 6a and b, respectively. The annealed and un-annealed particles of manganese oxide have different shapes, and that the particle size of manganese oxide decreases with annealing. This phenomenon is attributable to the vaporization of water molecules (from the O 1s data in Table 3, after annealing, the amount of H–O–H decreased from 23.21% to 5.42%) and the reconstruction of manganese oxide during annealing. Therefore, following the annealing treatment, the manganese oxide particle size decreases. This probably leads to increase of specific area, potentially electroactive sites and specific capacitance. Thus, the SEM results confirm the specific capacitance data shown in Fig. 3.

X-ray diffraction patterns of electrodes with annealing at various temperatures (130, 160, and 195 °C) together with that for activated carbon are shown in Fig. 7. Comparing curves (1–3), all XRD patterns had broadened peaks with very low intensity (Mn_2O_3 Crystals of the electrodes with annealing at 160 °C and 130 °C) except the strong diffraction peaks associated with the electrode annealed at 195 °C. The major peaks in curve (1) of Fig. 7 are identified as coming from MnO_2 crystals.

In order to investigate the oxidation state of manganese oxide, XPS was used to examine the binding energy without annealing and with annealing at 195 °C. XPS spectral data of Mn $2p_{3/2}$, Mn 3s, and O 1s are listed in Table 3. The oxidation state of manganese oxide was determined by the differences of binding energy between the splitting peaks of Mn 3s in Table 3. The difference in binding energy changed from 5.44 to 4.82 eV following annealing. Thus, manganese oxide before annealing mainly

Table 3 XPS Mn $2p_{3/2}$, Mn 3s, and O ls binding energies (eV), differences of binding energies (eV), bands, and areas (%) for manganese oxide without annealing and with annealing at 195 °C

Sample	Mn $2p_{3/2}$	Mn 3 s			O ls		
	Eb (eV)	Eb(1) (eV)	Eb(2) (eV)	ΔE (eV)	Band	Eb (eV)	Area (%)
Without annealing	641.5	83.32	88.76	5.44	Mn–O–Mn	529.79	42.18
					Mn–OH	530.92	34.63
					H–O–H	532.0	23.21
With annealing	642.6	83.78	88.6	4.82	Mn–O–Mn	529.88	81.43
					Mn–OH	531.12	13.14
					H–O–H	532.17	5.42

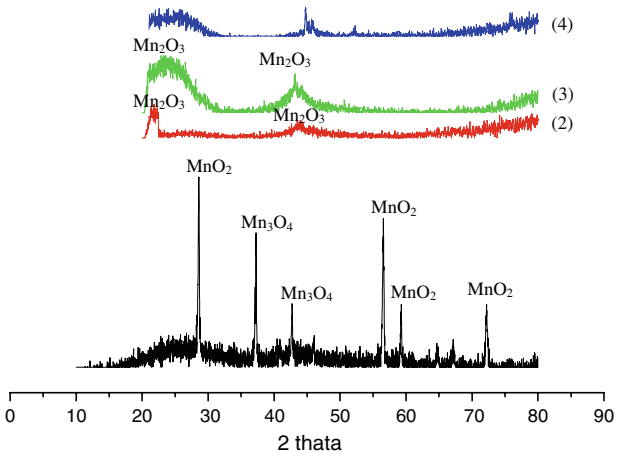

Fig. 7 X-ray diffraction patterns of electrodes after annealing at various temperatures [195 °C (1), 160 °C (2), and 130 °C (3)] and activated carbon (4)

consists of Mn^{3+} species and after annealing mainly consists of Mn^{4+} species [22]. In addition, from the O 1s data in Table 3, after annealing, the amount of Mn–O–Mn (oxide oxygen) increased from 42.18% to 81.43%, the Mn–OH (hydroxide) decreased from 34.63% to 13.14%, and the H–O–H (water) decreased from 23.21% to 5.42%. These results reveal that manganese oxide species are transformed from hydroxide to oxide—which represents the main species after annealing.

4 Conclusion

Maximum capacitance of 461.3 F g^{-1} was obtained at a scan rate of 25 mV s^{-1} in 0.1 M Na_2SO_4 electrolyte for manganese oxide prepared under the following optimum conditions: pH = 13.11 & T = 25 °C and annealed under the conditions: T = 195 °C. In addition, the smallest effective diameter of manganese oxide sol prepared under these conditions gives the highest specific capacitance. From CP results, charge–discharge curves were shown to be symmetrical and similar. This demonstrates high reversibility. Furthermore, XPS results indicated that the valence of manganese oxide increased and SEM revealed that the particle size decreased after annealing.

References

1. Conway BE (1999) Electrochemical supercapacitors – scientific fundamentals and technological applications. Kluwer Academic/Plenum Publishers, New York
2. Kotz R, Carlen M (2000) Electrochim Acta 45:2483
3. Chang JK, Tsai WT (2003) J Electrochem Soc 150:A1333
4. Chen YS, Hu CC (2003) Electrochem Solid-State Lett 6:A210
5. Jeong YU, Manthiram A (2002) J Electrochem Soc 149:A1419
6. Hu CC, Wang CC (2003) J Electrochem Soc 150:A1079
7. Park HP, Park OO, Shin KH et al (2002) Electrochem Solid-State Lett 5:H7
8. Reddy RN, Reddy RG (2003) J Power Sources 124:330
9. Burke A (2000) J Power Sources 91:37
10. Chang JK, Lin CT, Tsai WT (2004) Electrochem Commun 6:666
11. Hong MS, Lee SH, Kim SW (2002) Electrochem Solid-State Lett 5:A227
12. Park JH, Ko JM, Park OO (2003) J Electrochem Soc 150:A864
13. Zhang JR, Chen B, Li WK et al (2002) Int J Mod Phys B 16:4479
14. Zheng JP (1999) Electrochem Solid-State Lett 2:359
15. Pang SC, Anderson MA, Thomas WC (2000) J Electrochem Soc 147:444
16. Lee HY, Kim SW, Lee HY (2001) Electrochem Solid-State Lett 4:A19
17. Mulvaney P, Cooper R, Grieser F (1990) J Phys Chem 94:8339
18. Bordi F, Cametti C, Motta A (2000) J Phys Chem B 104:5318
19. Endo M, Maeda T, Takeda T et al (2001) J Electrochem Soc 148:A910
20. Dean JA, Lange NA (1973) Lange's handbook of chemistry, 8.164. McGraw-Hill, New York
21. Sostaric JZ, Mulvaney P, Grieser F (1995) J Chem Soc Faraday Trans 91:2843
22. Chigane M, Ishikawa M (2000) J Electrochem Soc 147:2246